

PAPER

# Trion-Facilitated Dexter-Type Energy Transfer in a Cluster of Single Perovskite CsPbBr<sub>3</sub> Nanocrystals<sup>\*</sup>

To cite this article: Zengle Cao *et al* 2020 *Chinese Phys. Lett.* **37** 127801

View the [article online](#) for updates and enhancements.

## Trion-Facilitated Dexter-Type Energy Transfer in a Cluster of Single Perovskite CsPbBr<sub>3</sub> Nanocrystals

Zengle Cao(曹增乐)<sup>1</sup>, Fengrui Hu(胡逢睿)<sup>2\*</sup>, Zaiqin Man(满再琴)<sup>2</sup>, Chunfeng Zhang(张春峰)<sup>1</sup>, Weihua Zhang(张伟华)<sup>2\*</sup>, Xiaoyong Wang(王晓勇)<sup>1\*</sup>, and Min Xiao(肖敏)<sup>1,3</sup>

<sup>1</sup>National Laboratory of Solid State Microstructures, Collaborative Innovation Center of Advanced Microstructures, and School of Physics, Nanjing University, Nanjing 210093, China

<sup>2</sup>College of Engineering and Applied Sciences, Nanjing University, Nanjing 210093, China

<sup>3</sup>Department of Physics, University of Arkansas, Fayetteville, Arkansas 72701, USA

(Received 15 September 2020; accepted 12 October 2020; published online 8 December 2020)

Semiconductor colloidal nanocrystals (NCs) can interact with each other to profoundly influence the charge transfer, transport and extraction processes after they have been assembled into a high-density film for optoelectronic device applications. These interactions normally occur among several nearby single colloidal NCs, which should be effectively separated from their surroundings to remove the ensemble average effect for fine optical characterizations. By means of atomic force microscopy (AFM) nanoxerography, here we prepare individual clusters of perovskite CsPbBr<sub>3</sub> NCs and perform single-particle measurements on their optical properties at the cryogenic temperature. While discrete photoluminescence bands can be resolved from the several single CsPbBr<sub>3</sub> NCs that are contained within an individual cluster, the shorter- and longer-wavelength bands are dramatically different in that their intensities show sub- and superlinear dependences on the laser excitation powers, respectively. This can be explained by the generation of charged excitons (trions) at high laser excitation powers, and their subsequent Dexter-type energy transfer from smaller- to larger-sized CsPbBr<sub>3</sub> NCs. Our findings not only suggest that these individual clusters prepared by AFM nanoxerography can serve as a potent platform to explore few-NC interactions but they also reveal the long-neglected role played by trions in channeling photo-excited energies among neighboring NCs.

PACS: 78.67.Bf, 71.35.Pq, 78.55.-m, 36.40.Vz

DOI: 10.1088/0256-307X/37/12/127801

Semiconductor perovskite nanocrystals (NCs) have been subjected to intensive optical characterizations that aim to explore their fundamental photophysical properties, since their first synthesis in 2015.<sup>[1,2]</sup> At the ensemble level, very rich research topics are currently being covered, ranging from ultrafast exciton dynamics,<sup>[3,4]</sup> carrier-phonon coupling,<sup>[5]</sup> amplified spontaneous emission,<sup>[6]</sup> energy transfer<sup>[7]</sup> to the novel ion migration<sup>[8]</sup> and superfluorescence<sup>[9]</sup> effects. At the single-NC level, the quantum-emitter feature has been confirmed from the single-photon emission measurements,<sup>[10,11]</sup> with the subsequent revelations of fluorescence blinking,<sup>[12,13]</sup> exciton fine structure<sup>[14–16]</sup> and coherent optical property.<sup>[17,18]</sup> Concomitant with the ever-increasing fundamental understandings of perovskite NCs, they have been implemented in a variety of practical applications, such as solar cells,<sup>[19,20]</sup> light-emitting diodes,<sup>[21]</sup> lasers<sup>[22]</sup> and photodetectors.<sup>[23]</sup> In these optoelectronic devices, perovskite NCs are unavoidably assembled into high-density films, where their mutual interactions are decisive in optimizing or deteriorating the relevant op-

eration parameters. It is obvious that neither the ensemble nor the single-NC approach is capable of precisely resolving these fine mutual interactions that normally occur among several neighboring perovskite NCs, which are difficult to be isolated out from the as-prepared solid films.

A viable solution of this problem is to prepare an individual cluster that contains a limited number of closely packed NCs, which was realized in several previous reports by focusing on the traditional CdSe system. By mixing methanol with hexane to change the solvent polarity, Yu and Van Orden demonstrated that several single CdSe/ZnS NCs could be clustered together with enhanced fluorescent blinking that might be caused by their collective charge interactions.<sup>[24]</sup> Under the condition of limited ligand protection, a flower-like cluster of 4–5 single CdSe/CdS NCs was synthesized by Zhang *et al.*, which was shown to still possess a photon-antibunching behavior arising from Auger interactions among their photogenerated excitons.<sup>[25]</sup> Cui *et al.* linked two single CdSe/CdS NCs with tetrathiol molecules and then fused them

Supported by the National Key R&D Program of China (Grant Nos. 2019YFA0308704 and 2017YFA0303700), the National Natural Science Foundation of China (Grant Nos. 61974058, 11574147 and 11621091), and the PAPD of Jiangsu Higher Education Institutions.

\*Corresponding authors. Email: frhu@nju.edu.cn; zwh@nju.edu.cn; wxiaoyong@nju.edu.cn

© 2020 Chinese Physical Society and IOP Publishing Ltd

via constrained oriented attachment to yield a dimer cluster, wherein the coherent coupling and wavefunction hybridization led to a redshift of the bandgap energy.<sup>[26]</sup> Very recently, Sharma *et al.* observed that individual clusters of perovskite CsPbBr<sub>3</sub> NCs could be formed in the emission layer of a light-emitting diode, and the electroluminescence (EL) primarily originated from larger-sized CsPbBr<sub>3</sub> NCs, due to efficient charge migration from smaller-sized CsPbBr<sub>3</sub> NCs.<sup>[27]</sup> Owing to the random formation feature, it was difficult in this case to achieve a systematic control over the size of an individual cluster, which could contain tens to hundreds of single CsPbBr<sub>3</sub> NCs, to give a succinct interpretation of their mutual interactions.

In this work, we employ atomic force microscopy (AFM) nanoxerography to deposit individual clusters of perovskite CsPbBr<sub>3</sub> NCs onto the sample substrate, the number of which can be well controlled by vary-

ing the voltage applied to the AFM tip. From optical measurements on individual clusters at the cryogenic temperature, discrete photoluminescence (PL) peaks can be well resolved from the neutral excitons of different single CsPbBr<sub>3</sub> NCs. With the increasing power of laser excitation on an individual cluster, the PL intensities of larger-sized CsPbBr<sub>3</sub> NCs show a super-linear dependence and become dominant over those of smaller-sized CsPbBr<sub>3</sub> NCs with a sublinear dependence. From optical measurements on single isolated CsPbBr<sub>3</sub> NCs, this superlinear dependence on the laser excitation power is also reflected in the PL intensities of charged excitons (trions). We thus propose that there should exist Dexter-type energy transfer from smaller- to larger-sized CsPbBr<sub>3</sub> NCs within an individual cluster, which is facilitated by the increasing probability of trion generation at higher laser powers.

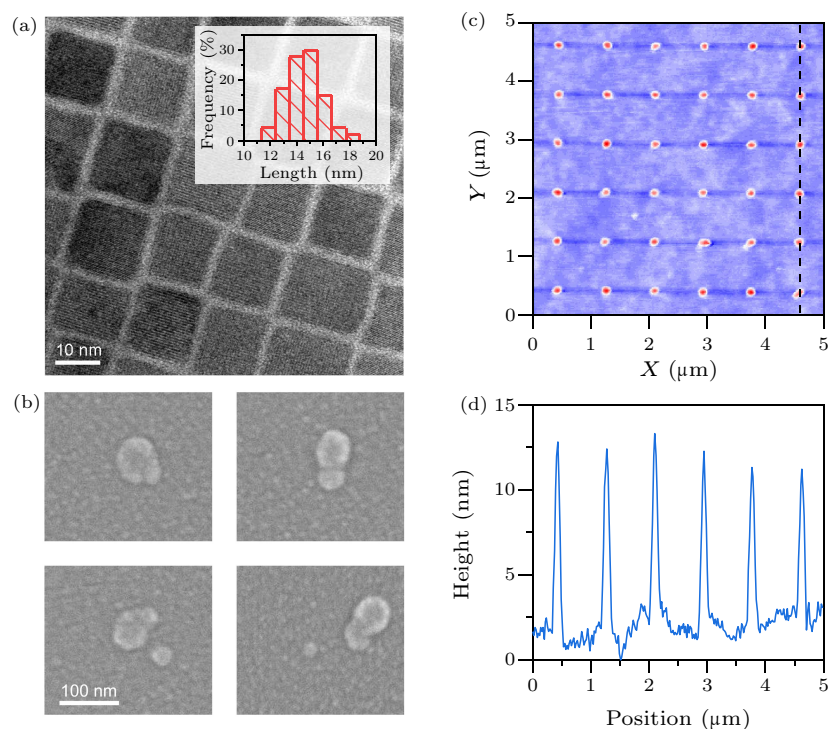


**Fig. 1.** (a) Transmission electron microscopy image of CsPbBr<sub>3</sub> NCs. Inset: statistic histogram for the size distribution of CsPbBr<sub>3</sub> NCs. (b) Scanning electron microscopy images of four individual clusters of CsPbBr<sub>3</sub> NCs. (c) Atomic force microscopy image of an array of individual clusters of CsPbBr<sub>3</sub> NCs. (d) Topographic height profile of individual clusters taken along the vertical dashed line in panel (c).

**Results.** By means of the hot injection method that has been reported before,<sup>[15]</sup> the colloidal CsPbBr<sub>3</sub> NCs are synthesized with an edge length of  $14.5 \pm 1.4$  nm [Fig. 1(a)], which is significantly larger than the exciton Bohr diameter of  $\sim 7$  nm to imply a weak quantum confinement.<sup>[1]</sup> To prepare individual clusters of CsPbBr<sub>3</sub> NCs with the AFM nanoxerography method,<sup>[28]</sup> a 100-nm-thick fluoropolymer film unwettable to cyclohexane is first spin-coated onto a Si substrate. Then a voltage ranging from 30 to 70 V

is applied to the AFM tip for the injection of charges into the fluoropolymer film. When the CsPbBr<sub>3</sub> NCs dissolved in a cyclohexane solution are spin-coated onto the fluoropolymer film, they can interact with the charges electrostatically to form local clusters. By moving the AFM tip and changing the applied voltage, the location of a cluster and the number of single CsPbBr<sub>3</sub> NCs therein can be well controlled. As shown in the scanning electron microscopy (SEM) image that is given in Fig. 1(b), the individual clusters

studied in our experiment are each characterized with a lateral size of  $\sim 62 \pm 13$  nm. Meanwhile, the AFM image measured for an array of individual clusters is plotted in Fig. 1(c), from which an average vertical height of  $\sim 12$  nm can be estimated for each cluster [Fig. 1(d)]. Based on these lateral size and vertical height measurements, it can be deduced that there are at most 10 single CsPbBr<sub>3</sub> NCs dwelling inside an individual cluster.

For comparison purposes, we have also prepared a solid film of isolated single CsPbBr<sub>3</sub> NCs by spin-coating one drop of their diluted cyclohexane solution onto a fused SiO<sub>2</sub> substrate. The sample substrate containing either individual clusters or isolated single CsPbBr<sub>3</sub> NCs is attached to the cold finger of a helium-free cryostat operated at 4 K, where they are excited at 405 nm by a picosecond pulsed laser with a repetition rate of 80 MHz. A dry objective with a numerical aperture of 0.82 is used to focus the laser beam, as well as to collect the PL signal, which is sent through a spectrometer to either a CCD for the PL spectral measurement or to an avalanche photodiode for the PL lifetime measurement with a resolution of  $\sim 100$  ps. To avoid possible generation of multiple excitons that might complicate the experimental results, all of the optical measurements are performed at the linear excitation regime so that the PL intensity of a single CsPbBr<sub>3</sub> NC increases linearly with the increasing laser power.

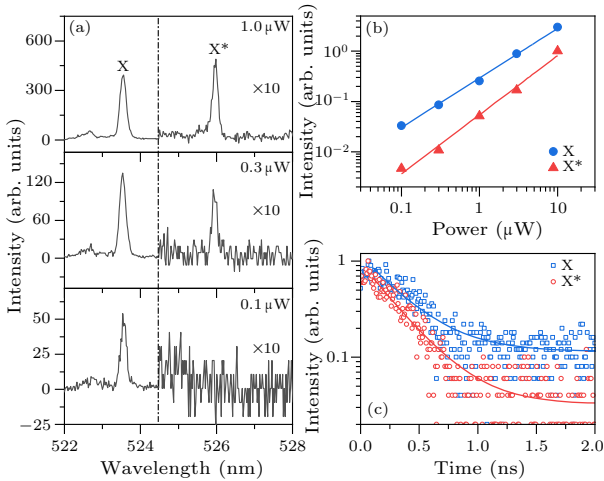


**Fig. 2.** (a) PL spectra of a single CsPbBr<sub>3</sub> NC measured at three different laser excitation powers. (b) PL intensities of neutral exciton (X, blue dots) and trion (X\*, red triangles) measured for this single CsPbBr<sub>3</sub> NC as a function of the laser excitation power, and fitted by the solid lines with power-law functions. (c) PL decay curves measured for neutral exciton (X, blue square) and trion (X\*, red circle) of this single CsPbBr<sub>3</sub> NC, and fitted by the solid lines with single-exponential functions.

The typical PL spectra measured for an isolated single CsPbBr<sub>3</sub> NC are plotted in Fig. 2(a), where only a single peak ( $\sim 523.5$  nm) exists at the low laser

power of  $0.1 \mu\text{W}$ , due to the optical emission of neutral exciton. With the increasing laser power, there emerges a new PL peak ( $\sim 526.0$  nm) from charged exciton (trion) whose recombination energy is  $\sim 11$  meV smaller than that of neutral exciton. As shown in Fig. 2(b), the PL intensities ( $I$ ) measured for neutral exciton at different laser powers ( $P$ ) can be fitted by the power-law function of  $I = P^n$  to yield a sublinear exponent of  $n = 0.99$ . Nevertheless, the trion PL intensity shows a superlinear behavior with an exponent of  $n = 1.17$ , which is consistent with the previous reports that the fast charging and discharging events would be triggered at high laser excitation powers.<sup>[13]</sup> The PL decay curves that are measured for neutral exciton and trion of this specific CsPbBr<sub>3</sub> NC are plotted in Fig. 2(c), which can be both fitted by single-exponential functions with the PL lifetimes of  $\sim 0.32$  and  $\sim 0.29$  ns, respectively. From the optical measurements on tens of single isolated CsPbBr<sub>3</sub> NCs, it can be concluded for the trion that its PL peak never appears at the low laser power of  $0.1 \mu\text{W}$ , its PL intensity always increases superlinearly with the laser power, and its PL lifetime is relatively shorter than that of the corresponding neutral exciton.

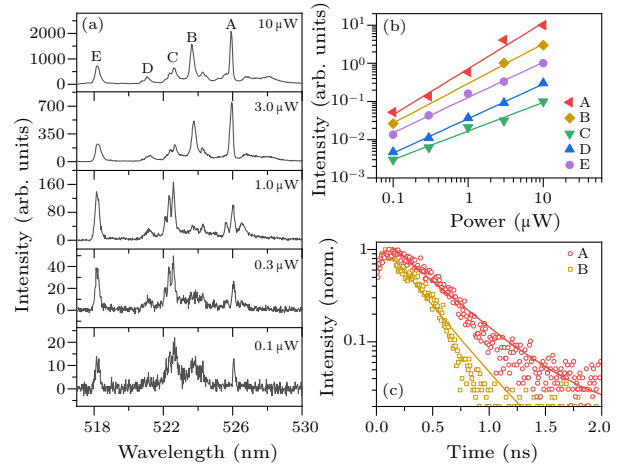


**Fig. 3.** (a) PL spectra measured for an individual cluster of CsPbBr<sub>3</sub> NCs at five different laser excitation powers, showing the existence of five emission bands marked by A, B, C, D and E, respectively. (b) PL intensities measured for these bands versus the laser excitation power, and fitted by the solid lines with power-law functions. (c) PL decay curves measured for the A and B bands, and fitted by the solid lines with single-exponential functions.

In the next experiment, we switch to the optical studies of individual clusters to probe possible interactions among the composing CsPbBr<sub>3</sub> NCs. As shown representatively in Fig. 3(a) for an individual cluster excited at increasing laser powers, five PL bands from different single CsPbBr<sub>3</sub> NCs can be roughly resolved, which are marked by A, B, C, D and E from the longer to shorter wavelengths. At the low laser power of  $0.1 \mu\text{W}$ , nearly all of these bands are present with comparable PL intensities. When the laser power is

further increased, it is surprising to see that PL intensities of the longer-wavelength bands become significantly dominant over those of the shorter wavelengths. From power-law fitting of the PL intensity as a function of the laser power [Figure 3(b)], the shorter-wavelength C, D and E bands are associated with sublinear exponents of 0.75, 0.90 and 0.92, respectively. In contrast, the respective exponents of 1.21 and 1.04 fitted for the longer-wavelength A and B bands are reminiscent of the superlinear PL behavior demonstrated in Fig. 2(b) for the trion. Since the A band has a more prominent superlinear dependence on the laser power than the B band, we will focus on it in the following discussions to explain the relevant PL mechanisms.

As mentioned earlier in the text, the A band already shows up at the laser power of  $0.1 \mu\text{W}$ , and

therefore it should originate from neutral exciton instead of trion that appears only at high laser powers. Meanwhile, it can be clearly seen that the A band is composed of triplet PL peaks especially at the laser power of  $1.0 \mu\text{W}$ , which should correspond to the fine energy-level structures of neutral exciton commonly observed in single perovskite NCs.<sup>[16,29]</sup> Meanwhile, a single PL peak should be expected from the trion emission due to the removal of electron-hole exchange interactions.<sup>[15]</sup> The PL lifetime measured for the A band is  $\sim 0.41 \text{ ns}$  [Fig. 3(c)], which is obviously longer than that of  $\sim 0.28 \text{ ns}$  for the B band, as well as those values for all the other bands in Fig. 3(a). This again excludes the possibility of trion emission from the A band, in which case its corresponding band (B, C, D or E) from neutral exciton should have a longer PL lifetime.

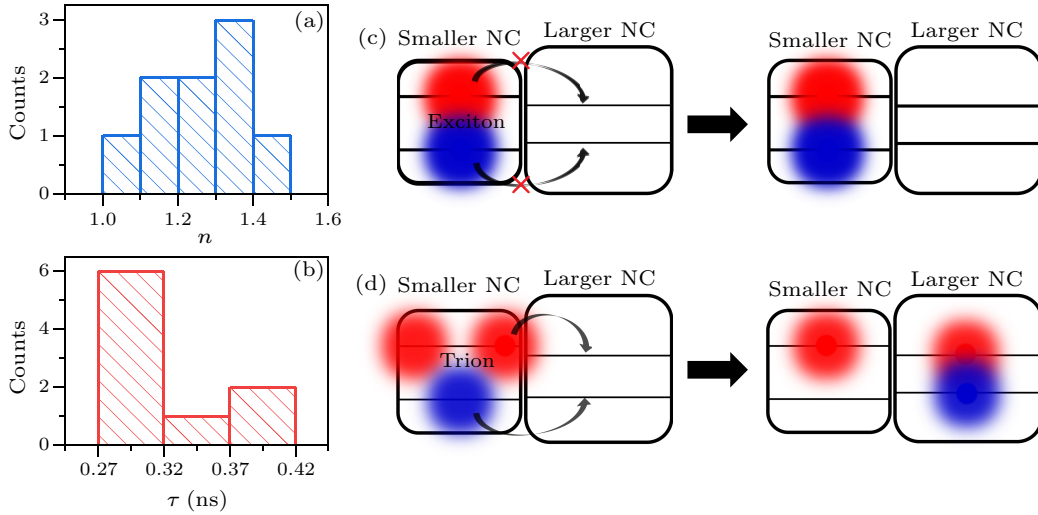


**Fig. 4.** (a) Statistic histogram showing the distribution of power-law fitting exponents ( $n$ ) for the laser-power-dependent PL intensities of the longer-wavelength bands in  $\sim 10$  individual clusters. (b) Statistic histogram showing the distribution of PL lifetimes ( $\tau$ ) measured for the longer-wavelength bands in  $\sim 10$  individual clusters. (c) At low laser power, the energy transfer via exciton migration among NCs is inefficient. (d) At high laser power, the trion presence facilitates Dexter-type energy transfer from smaller- to larger-sized NCs.

The trion-like feature, manifested as a superlinear dependence of the PL intensity on the laser excitation power, has been universally observed in the longer-wavelength bands emitted by individual clusters studied in our experiment. In Fig. 4(a), we plot a distribution histogram of the fitted power-law exponents  $n$  for the longer-wavelength bands from  $\sim 10$  individual clusters, which are all larger than one with an average value of  $\sim 1.25$ . The distribution of PL lifetimes measured for these longer-wavelength bands is plotted in the histogram of Fig. 4(b), which range from  $\sim 0.28$ – $0.41 \text{ ns}$  with an average value of  $\sim 0.32 \text{ ns}$  and a standard deviation of  $0.04 \text{ ns}$ . In contrast, the trion PL lifetimes measured for single isolated  $\text{CsPbBr}_3$  NCs are distributed within  $\sim 0.24$ – $0.28 \text{ ns}$  with an average value of  $\sim 0.26 \text{ ns}$  and a standard deviation of  $0.02 \text{ ns}$ . Based on the facts that the longer-wavelength bands originate from neutral excitons and

their PL intensities carry a trion-like feature in the laser-power dependence, we propose that, compared to the inactive energy transfer via exciton migration [Fig. 4(c)], there should exist trion-facilitated energy transfer from smaller- to larger-sized single  $\text{CsPbBr}_3$  NCs within an individual cluster [Fig. 4(d)].

*Discussions.* In general, the colloidal NCs closely packed inside a solid film can interact with each other through the cascaded, Förster resonance and Dexter-type energy transfer (ET) processes.<sup>[30]</sup> The cascaded ET mechanism can be safely ruled out here since we are dealing with an individual cluster of several single  $\text{CsPbBr}_3$  NCs, so that the photons emitted by one NC cannot be efficiently reabsorbed by the others. The Förster resonance ET proceeds through dipole-dipole interaction, and its efficiency is critically determined by the spectral overlap, separation distance and spatial orientation of the donor and acceptor NCs. Since

these parameters are fixed for the single CsPbBr<sub>3</sub> NCs inside an individual cluster, it is obvious that the efficiency of Förster resonance ET should be independent of the laser excitation power. This is in contrast to what has been observed in our experiment, which shows that the PL intensities of larger-sized CsPbBr<sub>3</sub> NCs have a faster increase than those of smaller-sized ones with the increasing laser excitation power. We are naturally left with the Dexter-type ET for the interactions of single CsPbBr<sub>3</sub> NCs within an individual cluster, which is made possible by the increasing probability of trion generation at higher laser excitation powers.

In a Dexter-type ET process, the photo-excited charge carriers can migrate directly among neighboring fluorophores, owing to the electron-density overlap between the donor excited and the acceptor ground states.<sup>[30]</sup> This overlap can be reinforced by the weak quantum confinement of the as-synthesized single CsPbBr<sub>3</sub> NCs, which dictates an easy diffusion of charge carriers to the interfaces, as well as by the larger spatial extent and higher electron density possessed by trions relative to those of neutral excitons.<sup>[31,32]</sup> From statistical optical measurements on a large number of single isolated CsPbBr<sub>3</sub> NCs, the trion binding energy is estimated to range from ~6–14 meV with an average value of ~10 meV. Because of this large distribution of trion binding energies, it is feasible for the transition energies of trions and neutral excitons from, respectively, the smaller- and larger-sized CsPbBr<sub>3</sub> NCs to overlap with each other, especially under the influence of spectral diffusion effect that is greatly enhanced at high laser excitation powers. Meanwhile, the average binding energy of ~10 meV for trions is significantly smaller than that of ~19–62 meV obtained previously for neutral excitons in CsPbBr<sub>3</sub> NCs,<sup>[33]</sup> which can also play an important role in accelerating the Dexter-type ET process.<sup>[34]</sup> With all of these beneficial factors, it can be envisioned that the energies of trions can be efficiently channeled out of smaller-sized CsPbBr<sub>3</sub> NCs before their radiative recombination, leading to enhanced absorption cross sections of neutral excitons in larger-sized CsPbBr<sub>3</sub> NCs.

In summary, we have fabricated individual clusters of single CsPbBr<sub>3</sub> NCs by means of AFM nanoxerography, and observed from each cluster that PL intensities of the longer-wavelength bands have a super-linear dependence on the laser excitation power. We propose that there should exist Dexter-type ET from smaller- to larger-sized single CsPbBr<sub>3</sub> NCs, which is facilitated by the efficient generation of trions at high laser powers. It should be noted that these results are consistent with what has recently been observed from the electroluminescence studies of individual NC clusters, where the charge carriers could also migrate

from smaller- to larger-sized CsPbBr<sub>3</sub> NCs to yield a red-shifted emission peak.<sup>[27]</sup> Since the EL operation is featured with imbalanced electron and hole injections,<sup>[35–37]</sup> the formation of trions should promote efficient charge transfer, accumulation and recombination in larger-sized CsPbBr<sub>3</sub> NCs with smaller bandgap energies.<sup>[27]</sup> Thus, our current work has not only revealed the important role played by trions in the charge exchange process among neighboring perovskite NCs but it has also provided valuable information on judicious designs of their high-performance optoelectronic devices. Specifically, the charging effect can be positively employed in photodetector and photovoltaic applications to strengthen the charge transport and extraction functionalities, and it should be minimized to the lowest level for achieving highly efficient photon outputs from light-emitting diodes and laser devices.

## References

- [1] Protesescu L, Yakunin S, Bodnarchuk M I, Krieg F, Caputo R, Hendon C H, Yang R X, Walsh A and Kovalenko M V 2015 *Nano Lett.* **15** 3692
- [2] Zhang F, Zhong H, Chen C, Wu X G, Hu X, Huang H, Han J, Zou B and Dong Y 2015 *ACS Nano* **9** 4533
- [3] Makarov N S, Guo S, Isaienko O, Liu W, Robel I and Klimov V I 2016 *Nano Lett.* **16** 2349
- [4] Cannesson D, Shornikova E V, Yakovlev D R, Rogge T, Mitioglu A A, Ballottin M V, Christianen P C M, Lhuillier E, Bayer M and Biadala L 2017 *Nano Lett.* **17** 6177
- [5] Iaru C M, Geuchies J J, Koenraad P M, Vanmaekelbergh D and Silov A Y 2017 *ACS Nano* **11** 11024
- [6] Yakunin S, Protesescu L, Krieg F, Bodnarchuk M I, Nedelcu G, Humer M, De Luca G, Fiebig M, Heiss W and Kovalenko M V 2015 *Nat. Commun.* **6** 8056
- [7] de Weerd C, Gomez L, Zhang H, Buma W J, Nedelcu G, Kovalenko M V and Gregorkiewicz T 2016 *J. Phys. Chem. C* **120** 13310
- [8] Zhang H, Fu X, Tang Y, Wang H, Zhang C, Yu W W, Wang X, Zhang Y and Xiao M 2019 *Nat. Commun.* **10** 1088
- [9] Rainò G, Becker M A, Bodnarchuk M I, Mahrt R F, Kovalenko M V and Stöferle T 2018 *Nature* **563** 671
- [10] Park Y S, Guo S, Makarov N S and Klimov V I 2015 *ACS Nano* **9** 10386
- [11] Hu F, Zhang H, Sun C, Yin C, Lv B, Zhang C, Yu W W, Wang X, Zhang Y and Xiao M 2015 *ACS Nano* **9** 12410
- [12] Swarnkar A, Chulliyil R, Ravi V K, Irfanullah M, Chowdhury A and Nag A 2015 *Angew. Chem. Int. Ed.* **54** 15424
- [13] Zhang A, Dong C and Ren J 2017 *J. Phys. Chem. C* **121** 13314
- [14] Rainò G, Nedelcu G, Protesescu L, Bodnarchuk M I, Kovalenko M V, Mahrt R F and Stöferle T 2016 *ACS Nano* **10** 2485
- [15] Yin C, Chen L, Song N, Lv Y, Hu F, Sun C, Yu W W, Zhang C, Wang X, Zhang Y and Xiao M 2017 *Phys. Rev. Lett.* **119** 026401
- [16] Becker M A, Vaxenburg R, Nedelcu G, Sercel P C, Shabaev A, Mehl M J, Michopoulos J G, Lambrakos S G, Bernstein N, Lyons J L, Stöferle T, Mahrt R F, Kovalenko M V, Norris D J, Rainò G and Efros A L 2018 *Nature* **553** 189
- [17] Utzat H, Sun W, Kaplan A E K, Krieg F, Ginterseder M, Spokoiny B, Klein N D, Shulenberg K E, Perkinson C F, Kovalenko M V and Bawendi M G 2019 *Science* **363** 1068
- [18] Lv Y, Yin C, Zhang C, Yu W W, Wang X, Zhang Y and

- Xiao M 2019 *Nano Lett.* **19** 4442
- [19] Sanehira E M, Marshall A R, Christians J A, Harvey S P, Ciesielski P N, Wheeler L M, Schulz P, Lin L Y, Beard M C and Luther J M 2017 *Sci. Adv.* **3** eaao4204
- [20] Swarnkar A, Marshall A R, Sanehira E M, Chernomordik B D, Moore D T, Christians J A, Chakrabarti T and Luther J M 2016 *Science* **354** 92
- [21] Song J, Li J, Li X, Xu L, Dong Y and Zeng H 2015 *Adv. Mater.* **27** 7162
- [22] Wang Y, Li X, Song J, Xiao L, Zeng H and Sun H 2015 *Adv. Mater.* **27** 7101
- [23] Ramasamy P, Lim D H, Kim B, Lee S H, Lee M S and Lee J S 2016 *Chem. Commun.* **52** 2067
- [24] Yu M and Van O A 2006 *Phys. Rev. Lett.* **97** 237402
- [25] Lv B, Zhang H, Wang L, Zhang C, Wang X, Zhang J and Xiao M 2018 *Nat. Commun.* **9** 1536
- [26] Cui J, Panfil Y E, Koley S, Shamalia D, Waiskopf N, Remennik S, Popov I, Oded M and Banin U 2019 *Nat. Commun.* **10** 5401
- [27] Sharma D K, Hirata S and Vacha M 2019 *Nat. Commun.* **10** 4499
- [28] Palleau E, Sangeetha N M, Viau G, Marty J D and Ressler L 2011 *ACS Nano* **5** 4228
- [29] Tamarat P, Bodnarchuk M I, Trebbia J B, Erni R, Kovalenko M V, Even J and Lounis B 2019 *Nat. Mater.* **18** 717
- [30] Menke S M and Holmes R J 2014 *Energy & Environ. Sci.* **7** 499
- [31] Luo X, Lai R, Li Y, Han Y, Liang G, Liu X, Ding T, Wang J and Wu K 2019 *J. Am. Chem. Soc.* **141** 4186
- [32] Tisdale W A and Zhu X Y 2011 *Proc. Natl. Acad. Sci. USA* **108** 965
- [33] Yettapu G R, Talukdar D, Sarkar S, Swarnkar A, Nag A, Ghosh P and Mandal P 2016 *Nano Lett.* **16** 4838
- [34] Choi J J, Luria J, Hyun B R, Bartnik A C, Sun L, Lim Y F, Marohn J A, Wise F W and Hanrath T 2010 *Nano Lett.* **10** 1805
- [35] Bae W K, Park Y S, Lim J, Lee D, Padilha L A, McDaniel H, Robel I, Lee C, Pietryga J M and Klimov V I 2013 *Nat. Commun.* **4** 2661
- [36] Makarov N S, McDaniel H, Fuke N, Robel I and Klimov V I 2014 *J. Phys. Chem. Lett.* **5** 111
- [37] Lin X, Dai X, Pu C, Deng Y, Niu Y, Tong L, Fang W, Jin Y and Peng X 2017 *Nat. Commun.* **8** 1132